

Holographic Dark Energy from Fluid/Gravity Duality Constraint by Cosmological Observations

Behnam Pourhassan^a Alexander Bonilla^b Mir Faizal^c Everton M. C. Abreu^{b,d}

^a*School of Physics, Damghan University, Damghan, Iran*

^b*Departamento de Física, Universidade Federal de Juiz de Fora, 36036-330, Juiz de Fora, MG, Brazil*

^c*Irving K. Barber School of Arts and Sciences, University of British Columbia - Okanagan, Kelowna, BC V1V 1V7, Canada*

^c*Department of Physics and Astronomy, University of Lethbridge, Lethbridge, Alberta, T1K 3M4, Canada*

^d*Grupo de Física Teórica e Matemática Física, Departamento de Física, Universidade Federal Rural do Rio de Janeiro, 23890-971, Seropédica, RJ, Brazil*

E-mail: b.pourhassan@du.ac.ir, abonilla@fisica.ufjf.br,
f2mir@uwaterloo.ca, evertonabreu@ufrrj.br

ABSTRACT: In this paper, we obtain a holographic model of dark energy using the fluid/gravity duality. This model will be dual to a higher dimensional Schwarzschild black hole, and we would use fluid/gravity duality to relate to the parameters of this black hole to such a cosmological model. We will also analyze the thermodynamics of such a solution, and discuss the stability model. Finally, we use cosmological data to constraint the parametric space of this dark energy model. Thus, we will use observational data to perform cosmography for this holographic model based on fluid/gravity duality.

KEYWORDS: Black Hole, Fluid/Gravity Duality, Dark Energy, Cosmology, Cosmography.

Contents

1	Introduction	1
2	Fluid/Gravity	2
3	Holographic Dark Energy	5
4	Thermodynamics	7
5	Cosmology	8
5.1	Data Sets and Fitting Method	8
5.2	Cosmography	10
6	Conclusion	11
7	Acknowledgments	13

1 Introduction

The holographic principle states that the number of degrees of freedom in a region of space area equal to the degrees of freedom on the boundary of that region of space [1, 2]. The AdS/CFT correspondence is a concrete realization of the holographic principle, as it states that the string theory/supergravity on AdS space-time is dual to the superconformal field theory on the boundary of that of that AdS space-time [3–5]. An interesting part of the AdS/CFT correspondence is that it can establish a duality between weakly coupled theories and strongly coupled coupled theories. Thus, it has been used to study different aspects of strongly coupled theories which describe the quark-gluon plasma (QGP) [6–8], and this duality between the QCD and AdS is called AdS/QCD correspondence [9, 10]. This correspondence has been used to study the field theory dual to STU model as a theory which could describe such physical systems [11–13]. In fact, various properties of QGP have been studied using this duality with STU black hole [14–16]. The AdS/CFT correspondence has also been used to study condense matter systems, and this holographic description of the condensed matter systems is called the AdS/CMT correspondence [17–19]. In fact, certain deformations of the AdS backgrounds have been used to holographically analyze superfluid [20] and superconductor [21].

An interesting use of the AdS/CFT correspondence is that it can be used to holographically analyze the hydrodynamic description of strongly coupled conformal field theories [22]. This holographic description of the hydrodynamic description of strongly coupled conformal field theories is usually called the gauge/fluid duality. The fluid/gravity duality is important, as it is hoped that certain problems in the fluid mechanics such as the global

regular solutions of the Navier-Stokes equations and turbulence phenomena could be analyzed holographically using this duality. This duality can also be used to analyze fluids dual to certain black hole solutions. In fact, it has been proposed that a five dimensional Schwarzschild black hole is dual to an interesting fluid mechanical system, [23].

It has also been proposed that cosmological solution can be studied holographically using this fluid/gravity [24]. It has also been proposed that the dark energy of the universe can be studied holographically [25–28]. Holographic dark energy with massive neutrinos has also been studied and constraints using cosmological data from the Planck CMB lensing data, Planck CMB temperature data, the JLA supernova data, the baryon acoustic oscillation data, the cosmic shear data of weak lensing, the Hubble constant direct measurement, and the redshift space distortions data [29]. The interacting holographic dark energy models have been studied for various different interactions [30, 31]. It was observed that the type of interaction terms is constraint by the cosmological data for these interacting holographic dark energy models. Thus, it is important and interesting to study holographic models of dark energy. It may be noted that it is possible to use the fluid/gravity duality to holographically models of dark energy, and field the suitable gravity dual to such solutions. Thus, in this paper, we will analyze holographic dark energy using fluid/gravity duality. We will also use cosmological observations to constraint the parametric space of such a holographic model.

In this paper we follow method of the Ref. [32] to produce fluid equation of state, then compare it with the dark energy equation of state. Therefore, we can find time dependent black hole horizon and discuss about thermodynamics of the universe base on such fluid. The rest of paper is organized as follows. In the next section, we review some basic concept of fluid/gravity correspondence and obtain energy density and pressure corresponding to five dimensional Schwarzschild black hole. In section 3 we discuss about dark energy equation of state and relate it to the fluid studied in section 2. In the section 4 we study thermodynamics of the model and discuss about stability of the system. Finally, in section 5 we give conclusion and some proposal for the future works.

2 Fluid/Gravity

In this section we will review the fluid/gravity duality. We first noted that at long-wavelengths, the effective dynamics of a continuum system can be described using fluid mechanics. Furthermore, according to fluid/gravity duality, this fluid mechanical system on the boundary of an AdS space-time is dual to the bulk Einstein equations in the AdS space-time [33]. So, such a fluid mechanical system can be described by an asymptotically AdS space-time with the following action,

$$S = \frac{1}{2\kappa} \int d^5x \sqrt{-g} (R - 2\Lambda) + \dots, \quad (2.1)$$

where $\kappa = 8\pi G$, and dots denotes interaction and boundary terms. One possible solution to this action is the AdS-Schwarzschild black hole. We can write the metric for this solution

as

$$ds^2 = \frac{L^2}{r^2} \left(-f(r)dt^2 + \frac{dr^2}{f(r)} + dX^2 \right), \quad (2.2)$$

where L is the constant AdS radius, and dX^2 is the $d-2$ dimensional metric of the flat space ($dX^2 = dx_1^2 + dx_2^2 + dx_3^2$), in five dimensional case. Also, for the case of five dimensional AdS Schwarzschild black hole, we have,

$$f(r) = 1 - \frac{r^4}{r_h^4}, \quad (2.3)$$

where r_h is the radius of the event horizon for the black hole. The boundary for this space-time can be described by the generic hypersurface Q , such that it is parameterized by the function $y(r)$. The intrinsic stress-energy tensor for this system can be written as

$$T_{ab} = -\frac{L^3}{\kappa r^3} \left(K_{ab} - Kh_{ab} + \Sigma h_{ab} - \kappa T_{ab}^{(R)} - \kappa T_{ab}^{(ct)} \right), \quad (2.4)$$

where h_{ab} is induced metrics on Q , and Σ is tension of Q . Here K is the trace of the the extrinsic curvature K_{ab} . In this system, $T_{ab}^{(R)}$ and $T_{ab}^{(ct)}$ are additional possible contributions from the intrinsic curvature and counter-terms respectively. Using the boundary stress-energy tensor, the components of four dimensional boundary, can be written as

$$\rho = \frac{L^3}{2\kappa r^4} \left(2\Sigma L + \frac{(rf'(r) - 4f(r))y'(r) - 4f(r)^2y'(r)^3 + 2rf(r)y''(r)^2}{(1 + f(r)y'(r)^2)^{\frac{3}{2}}} \right), \quad (2.5)$$

$$p_T = \frac{L^3}{2\kappa r^4} \left(-2\Sigma L + \frac{2(2f(r) - rf'(r))y'(r) + f(r)(4f(r) - rf'(r))'y'(r)^3 - 2rf(r)y''(r)^2}{(1 + f(r)y'(r)^2)^{\frac{3}{2}}} \right), \quad (2.6)$$

$$p_L = \frac{L^3}{2\kappa r^4} \left(-2\Sigma L + \frac{y'(r)(4f(r) - rf'(r))}{(1 + f(r)y'(r)^2)^{\frac{1}{2}}} \right), \quad (2.7)$$

where ρ is energy density. Here p_T and p_L are transverse and longitudinal pressures, respectively. The prime denotes a derivative with respect to r . There are two transverse components, and one longitudinal component. In order to satisfy Neumann boundary conditions for $T_{ab} = 0$ one need to set $\Sigma = 0$ in the dimensions greater that three. In fact, it is required to set $\Sigma = 0$ to obtain a perfect fluid equation of state. It is also possible to set $\Sigma L = 2\cos\theta$, where θ is the angle of the hypersurface Q with the y -axis. In order to have fluid mechanical system, we require isotropic pressures, and so we have $p_T = p_L = p$, and obtain

$$\sqrt{f(r)}y'(r) = c, \quad (2.8)$$

where c is an integration constant. Thus, we can write

$$y - y_0 = c \int_0^r \frac{dr}{\sqrt{f(r)}}. \quad (2.9)$$

For the $f(r)$ given by the Eq. (2.3), we can solve above integration numerically and plot y in terms of r (see Fig. 1). Behavior of y is consistent with the results of the what is

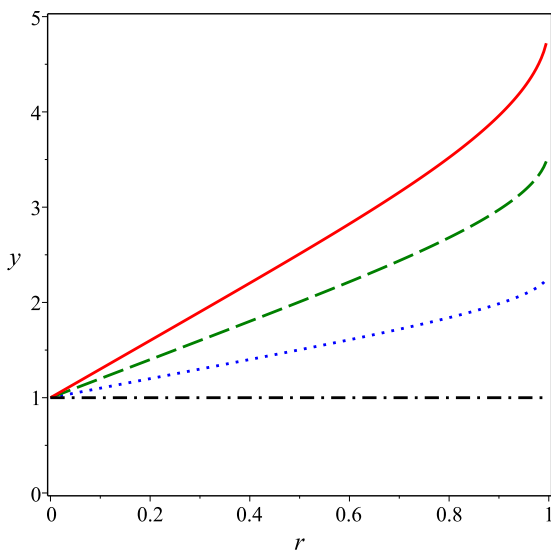


Figure 1. Profiles of the brane Q in terms of r for $y_0 = 1$ and $r_h = 1$. $c = 0$ (black dash dot), $c = 1$ (blue dot), $c = 2$ (green dash), $c = 3$ (red solid).

expected from a four dimensional Schwarzschild black hole [32]. Angle of curves with the black dash dot line are denoted by θ . In fact, as we have to only consider the positive value of c , so we have $c \geq 0$ [32]

If we assume $y(r_h) = y_h$, then we can write,

$$\tan \theta \approx \frac{\Delta y}{r_h}, \quad (2.10)$$

where $\Delta y = y_h - y_0$ is characteristic distance scale. In the special case of $r \ll r_h$ (close to boundary), we use the Taylor expansion and obtain,

$$y - y_0 \approx \frac{2^{\frac{1}{4}}}{2} cr_h \left[\tan^{-1} \frac{r}{2^{\frac{1}{4}} r_h} + \frac{1}{2} \ln \frac{r + 2^{\frac{1}{4}} r_h}{r - 2^{\frac{1}{4}} r_h} \right]. \quad (2.11)$$

Now we can write the energy density of this system as

$$\rho = \frac{L^3}{2\kappa r^4} \left(2\Sigma L + \frac{c(rf'(r) - 4f(r)) - 4c^3 f(r) - crf'(r)}{\sqrt{1 + c^2} \sqrt{f(r)}} \right). \quad (2.12)$$

We can also write the pressure of this system as

$$p = \frac{L^3}{2\kappa r^4} \left(-2\Sigma L - \frac{c(rf'(r) - 4f(r))}{\sqrt{1 + c^2} \sqrt{f(r)}} \right). \quad (2.13)$$

Now we will use this holographic description to understand a dark energy model, and holographically analyze such a model.

3 Holographic Dark Energy

In this section, we will use a holographic description to analyze a holographic model of dark energy dual to such a background geometry. So, here we will model dark energy with a perfect fluid, with energy density ρ and pressure p . The equation of state for this model of dark energy would be

$$\omega = \frac{p}{\rho}. \quad (3.1)$$

Now using Eqs. (2.12) and (2.13), we observe that for $\omega = -1$, we have the equation of state with a cosmological constant

$$p = -\rho = \frac{L^3}{2\kappa r^4} \left(-2\Sigma L + 4c\sqrt{1+c^2}\sqrt{f(r)} \right). \quad (3.2)$$

It may be noted that for the general case, we should set $\Sigma = 0$. Thus, comparing Eqs. (2.12) and (2.13), and using (3.1), we obtain

$$4(1 + (1 + c^2)\omega)f(r) = rf'(r). \quad (3.3)$$

Solution of this equation can be expressed as

$$f(r) = Ar^{4(1+(1+c^2)\omega)}, \quad (3.4)$$

where A is an integration constant.

This Friedmann equation in flat space for this dark energy model can be written as

$$H^2 = \frac{8\pi G}{3}\rho, \quad (3.5)$$

$H = \frac{\dot{a}}{a}$ is the Hubble's parameter and $a(t)$ is the scale factor. If this fluid is the dominant form of matter in a flat universe, then we can write

$$a = a_0 t^{\frac{2}{3(1+\omega)}}, \quad (3.6)$$

and so $H \propto t^{-1}$. If we set $A = -r_h^{-4}$, and assume that $r \gg r_h$, then we obtain

$$r_h = \sqrt{\frac{3}{2}}(1 + \omega)c_1 L^{\frac{3}{2}} \frac{t}{r_b}, \quad (3.7)$$

where c_1 is an arbitrary constant. Now r_b is the radius at which the fluid describes the dark energy, such that

$$Ar^{4(1+(1+c^2)\omega)} + r_h^{-4}r^4 = 1 \quad (3.8)$$

where r_b is the real positive root of this equation. It may be noted that we have now obtained a time-dependent black hole with the horizon given. Hence, we conclude that r_h is constant and r_b is time-dependent. So, r_b corresponds to time-dependent dark energy. Hence, we rewrite the Eq. (3.7) as

$$r_b = C \frac{t}{r_h}, \quad (3.9)$$

where $C \equiv (\sqrt{\frac{3}{2}}(1+\omega)c_1L^{\frac{3}{2}})^{-1}$ is a constant.

It may be noted that if we assume $1 + (1 + c^2)\omega = 2$, then it is possible to solve the Eq. (3.8) and obtain

$$r_b^4 = \frac{r_h^{-4}}{2A}(-1 + \sqrt{1 + 4Ar_h^8}). \quad (3.10)$$

If we set $c = \sqrt{2}$, we obtain $\omega = \frac{1}{3}$, and this is the equation of state of ultra-relativistic matter. This can represent radiation matter in the very early universe. For any value of positive A , we have $r_b \leq r_h$. For large values of r_h , we have $r_b \rightarrow 1$, and we can obtain time-dependent r_b as,

$$r_b = \sqrt{\frac{Ct}{1 + AC^4t^4}}, \quad (3.11)$$

where C is constant. So, at large t , r_b becomes a constant.

Now if $1 + (1 + c^2)\omega = \frac{1}{2}$, then we can solve Eq. (3.8) and obtain,

$$r_b^2 = \frac{Ar_h^4}{2}(-1 + \sqrt{1 + \frac{4r_h^{-4}}{A^2}}). \quad (3.12)$$

The expansion of the universe is accelerating for any equation of state $\omega < -\frac{1}{3}$. So, for any value of positive A , we have $r_b \leq r_h$. Now we can write the time-dependent radius as

$$r_b = (1 + \sqrt{1 + 64C^4t^4})^{\frac{1}{4}}. \quad (3.13)$$

In the large t limit, we obtain $r_b \propto t$. However, the energy density of this case is negative; hence it is un-physical.

Now for $1 + (1 + c^2)\omega = -1$, we can solve the Eq. (3.8) and obtain,

$$r_b^4 = \frac{r_h^4}{2}(1 \pm \sqrt{1 - 4Ar_h^{-4}}). \quad (3.14)$$

Here for $0 \leq c^2 \leq 1$, we have $\omega \leq -1$, and we get the hypothetical phantom energy and would cause a big rip. So, for any value of positive A , we have $r_b \leq r_h$. Now from Eq. (3.14), we obtain

$$r_b = \frac{1}{6}[216X(t) + \frac{2592C^4t^4}{X(t)}]^{\frac{1}{4}}, \quad (3.15)$$

where

$$X(t) = \left(-108AC^4t^4 + 12\sqrt{-12C^{12}t^{12} + 81A^2C^8t^8}\right)^{\frac{1}{3}}. \quad (3.16)$$

At the large t , we r_b becomes a constant, otherwise we get negative density.

In general, using the conditions given by Eqs. (3.3) and (3.8), we obtain ,

$$p = \omega\rho = \frac{2L^3c(1+c^2)\omega}{kr_b^4}f(r_b). \quad (3.17)$$

As discussed above, using explicit time-dependent r_b , and Eq. (3.6), we obtain

$$\rho = C_1a^{-6(1+\omega)} + \rho(0), \quad (3.18)$$

where $C_1 \equiv \frac{2L^3c(1+c^2)r_h^4}{ka_0^{-6(1+\omega)}}$ is a constant and $\rho(0)$ is initial density at $a = 0$. In this section, we model dark energy using a holographic fluid. In the next section, we will study thermodynamics of this holographic fluid representing the dark energy.

4 Thermodynamics

Now we can analyze the thermodynamics of this holographic dark fluid. We first observe that Eqs. (2.2) and (2.3) describe a black hole with the horizon radius r_h , and so we can write the Hawking temperature for this black hole as

$$T_H = \frac{1}{\pi r_h}. \quad (4.1)$$

Also the local temperature on the surface Q , which is given by

$$T = \frac{T_H}{\sqrt{f(r)}} = \frac{r_h}{\pi \sqrt{r_h^4 - r^4}}. \quad (4.2)$$

So, the local temperature where dual fluid describes the dark energy is

$$T_b = \frac{r_h}{\pi \sqrt{r_h^4 - r_b^4}}. \quad (4.3)$$

For the r_b near the boundary ($r_b \rightarrow 0$), the local temperature is equal to the Hawking temperature, $T_b = T_H$. The local entropy density for this system can be written as

$$s = \frac{p + \rho}{T}. \quad (4.4)$$

So, by using Eqs., (3.17) and (4.3), we obtain the entropy of the fluid corresponding to the dark energy,

$$s = 2\pi L^3 c(1 + c^2)(1 + \omega) \frac{(r_h^4 - r_b^4)^{\frac{3}{2}}}{r_b^4 r_h^5}. \quad (4.5)$$

To have positive entropy, we should have $\omega > -1$, otherwise it may produce phantom energy. It may be noted that with the current observational data, it is impossible to distinguish between phantom $\omega < -1$ and non-phantom $\omega \geq -1$. It is clear that the entropy density is constant on the surface, which is proportional to the area of the horizon swept by the hypersurface.

Now using the Eqs. (2.12), (2.13), and (4.4), we obtain

$$s(r = r_h) = \frac{2\pi L^3 c}{\sqrt{1 + c^2}} \frac{1}{r_h^3}, \quad (4.6)$$

which for the $c \gg 1$ produces the five dimensional Schwarzschild entropy.

Furthermore, using the Eq. (4.5), we obtain

$$F = - \int s dT, \quad (4.7)$$

and so we can write the free energy of the surface as

$$F = - \frac{L^3 c(1 + c^2)(1 + \omega)(r_b^4 - 4r_h^4 \ln r_h)}{2r_h^4 r_b^4}. \quad (4.8)$$

Now we can use the specific heat and speed of sound to study the stability of the model. The specific heat for this system can be written as

$$C_v = T \frac{\partial s}{\partial T}. \quad (4.9)$$

At the surface, $r = r_b$, so we obtain

$$C_v = -\frac{10\pi c(1+c^2)L^3(1+\omega)(r_b^4 + \frac{r_h^4}{5})(r_h^4 - r_b^4)^{\frac{3}{2}}}{r_h^5 r_b^4 (r_b^4 + r_h^4)}. \quad (4.10)$$

This specific heat is negative for $\omega > -1$. There is another test for stability of the model, and this test is based on the speed of sound,

$$v_s^2 = \frac{\partial p}{\partial \rho}. \quad (4.11)$$

For the fluid describing holographic dark energy, we have

$$v_s^2 = \omega. \quad (4.12)$$

So, if $\omega > 0$, we get $v_s^2 > 0$ and $C < 0$. However, if $\omega < -1$, then we get $C > 0$ and $v_s^2 < 0$. It is interesting to note that it is possible to the extended Chaplygin gas models equation of state [34–37],

$$p = -\frac{B}{\rho^\alpha} + A_1\rho + A_2\rho^2 + \dots. \quad (4.13)$$

and analyze the stability of such systems. It would be interesting to use such equations of states and analyze the stability of dark energy model using a dual description.

5 Cosmology

In this section, we briefly describe the observational data sets, the fitting method used to constrain the parameters of our model based on Friedmann equation (3.5) in the presence of an effective dark energy in the form of (3.18). A cosmography analysis the evolution of model also is presented in what follows.

5.1 Data Sets and Fitting Method

In order to constrains the free parameters of the models, we use i) The Union 2.1 sample [40], which contains 580 Supernovae type Ia (SNIa), and we fit the SNIa data by minimizing the χ^2 value as defined in [41]. ii) The baryon acoustic oscillations (BAO) measurements from WiggleZ BAO data, where the total χ^2 for all the BAO data sets have 3 data point ($\bar{A}_{obs} = (0.447, 0.442, 0.424)$ at $z = (0.44, 0.60, 0.73)$) from [42]. iii) We adopt also 36 Observational Hubble Data (Hz) at different redshifts ($0.0708 \leq z \leq 2.36$) obtained from [43], where 26 value are deduced from the differential age method, whereas 10 corresponds to that obtained from the radial BAO method. The χ^2 function for Hz is built as in [41].

Maximum likelihood \mathcal{L}_{max} , is the procedure of finding the value of one or more parameters for a given statistic which makes the known likelihood distribution a maximum. The maximum likelihood estimate for the best fit parameters p_i^m is

$$\mathcal{L}_{max}(p_i^m) = \exp \left[-\frac{1}{2} \chi_{min}^2(p_i^m) \right] \quad (5.1)$$

If $\mathcal{L}_{max}(p_i^m)$ has a Gaussian errors distribution, then $\chi_{min}^2(p_i^m) = -2 \ln \mathcal{L}_{max}(p_i^m)$, which is our case [44]. So, for our analysis $\chi_{min}^2 = \chi_{SNIa}^2 + \chi_{BAO}^2 + \chi_{H(z)}^2$. The Fisher matrix is widely used in the analysis of the constraint of cosmological parameters from different observational data sets [45, 46]. They encode the Gaussian uncertainties of the several parameters p_i . Given the best fit χ_{min}^2 , the Fisher matrix can be calculated as

$$F_{ij} = \frac{1}{2} \frac{\partial^2 \chi_{min}^2}{\partial p_i \partial p_j}, \quad (5.2)$$

where p_i and p_j are the set of free parameters in each cosmological model. The inverse of the Fisher matrix is the covariance matrix $[C_{cov}] = [F]^{-1}$, where the uncertainties are obtained as $\sigma_i = \sqrt{Diag[C_{cov}]_{ij}}$.

Figure (2) shows the 68.27% and 95.45% regions of statistical confidence in the plane $(\Omega_{m0} - w)$ considering the observational data from $H(z)$, $H(z) + SNIa$ and $H(z) + SNIa + BAO$. Note that these results are in agreement with Λ CDM model, which is obtained for $w = -1$ is inside the obtained region. On the other hand, the equation of state (EoS) can help us to classify the model as phantom if EoS $w < -1$, or as quintessence if $w > -1$. Here, we note that the EoS is closed at $w = -1$ for all combinations of data. But, the introduction of $SNIa + BAO$ on $H(z)$ causes small variation into direction to a possible phantom dynamic. In all combinations of data, although within the margin of error this cannot yet be still discriminated. Table 1 summarize the main results of the statistical analysis, and we can notice that although the value of χ_{min}^2 for $H(z)$ is a little below 36, this is greatly improved when the other data sets are introduced. Hence in summary, it is clear that Fluid/Gravity model, under all the above three different combinations of statistical data sets, remains close to Λ CDM cosmology.

Data	h	Ω_m	w	χ_{min}^2
$H(z)$	0.698 ± 0.042	0.254 ± 0.021	-0.972 ± 0.111	17.151
$H(z)+SNIa$	0.687 ± 0.013	0.256 ± 0.017	-0.973 ± 0.029	579.484
$H(z)+SNIa+BAO$	0.693 ± 0.012	0.270 ± 0.014	-0.994 ± 0.025	581.293

Table 1. Summary of the best fit values at 1σ of the free parameters (h , Ω_m , w) to Fluid/Gravity model, for three different observational data sets with χ_{min}^2 .

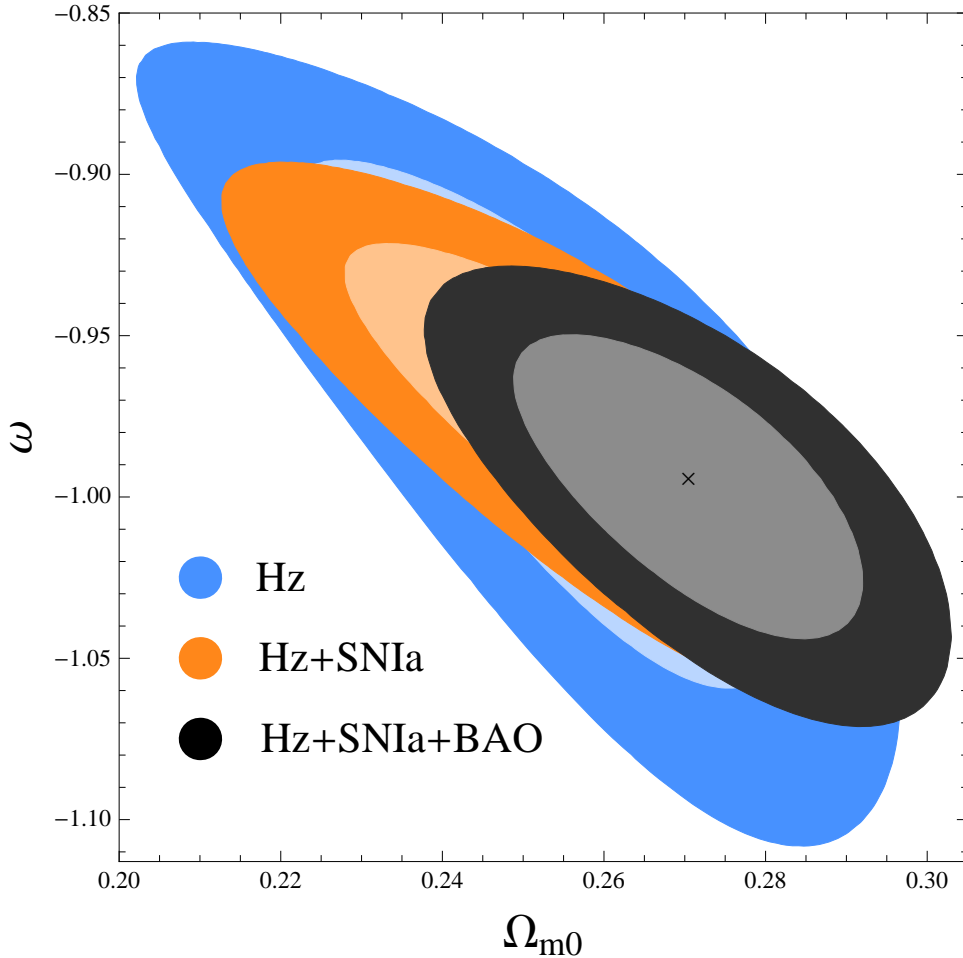


Figure 2. 1σ and 2σ confidence regions of the Fluid/Gravity model obtained from the joint analysis $H(z)$, $H(z) + \text{SNIa}$ and $H(z) + \text{SNIa} + \text{BAO}$ for the free parameters (h, Ω_m, w) .

5.2 Cosmography

It is natural to describe the kinematics of the cosmic expansion through the Hubble parameter $H(t)$ and its derivatives cosmographic parameters. Following to [47] the scale factor $a(t)$ expands into a Taylor series around the current time (t_0) as

$$\frac{a(t)}{a(t_0)} = 1 + \frac{H_0}{1!} [t - t_0] - \frac{q_0}{2!} H_0^2 [t - t_0]^2 + \frac{j_0}{3!} H_0^3 [t - t_0]^3, \quad (5.3)$$

where in general we can have a kinematic description of the cosmic expansion through the set of parameters

$$H(t) \equiv \frac{1}{a} \frac{da}{dt}; \quad q(t) \equiv -\frac{1}{a} \frac{d^2 a}{dt^2} H(t)^{-2}; \quad j(t) \equiv \frac{1}{a} \frac{d^3 a}{dt^3} H(t)^{-3}, \quad (5.4)$$

where the last term is known as jerk parameter $j(t)$. The big advantage of this method is that we can investigate the cosmic expansion without assuming any modification of gravity

theory or dark energy model due to its geometrical approach. The dependence between the free parameters of Fluid/Gravity model and the kinematic parameters $H(z)$, $q(z)$ and $j(z)$ can be obtained from the equations (3.5) and (3.18) as

$$H(z) = H_0 \left(\Omega_{r0}(1+z)^4 + \Omega_{m0}(1+z)^3 + \Omega_X(z) \right)^{1/2}, \quad (5.5)$$

where $\Omega_X(z) = (1 - \Omega_{m0} - \Omega_{r0})(1+z)^{6(1+w)}$ and $\Omega_X(z) = \rho(z)/\rho_{cri}$ is given by equation (3.18), $\rho_{cri} = 3H_0^2/8\pi G$ is critical density, Ω_{r0} and Ω_{m0} are radiation and matter density respectively, and w is the EoS. Here, we have that $\Omega_{r0}(h) = \Omega_\gamma(h)(1 + 0.2271N_{eff})$, where $\Omega_\gamma(h) = 2.46910^{-5}h^{-2}$ is the density of photons, $N_{eff} = 3.046$ is the effective number of neutrino species [38], and $h = H_0/100\text{kms}^{-1}\text{Mpc}^{-1}$ is dimensionless Hubble parameter. Thus, our model has 3 parameters free $\{h, \Omega_{m0}, w\}$, whose fit with the observational data is shown in Table 1. The deceleration and jerk parameters [39] are obtained as

$$q(z) = -1 + \frac{(1+z)}{H(z)} \frac{dH(z)}{dz}; \quad j(z) = q^2 + \frac{(1+z)^2}{H(z)} \frac{d^2H(z)}{dz^2}. \quad (5.6)$$

In order to characterize whether the universe is currently accelerated or decelerated, the history of expansion is fit through deceleration parameter $q(z)$. If $q(z) > 0$, $\ddot{a}(z) < 0$; then the expansion decelerate, as expected due to gravity (i.e. dark matter, baryonic matter, radiation). In general, if $\Omega_X \neq 0$ is sufficiently large (i.e. $\Omega_X > \Omega_m$), then $q(z) < 0$ and $\ddot{a}(z) > 0$, which corresponds to an expansion accelerated the universe as shown by observational data at present (see Figure (4)).

Figure (3) shows the evolution of $H(z)$ obtained in our analysis with propagation of error to 1σ (gray region) obtained from the best fit of parameters with all observational data, which seems agree with this data set. Figure (4) shows the deceleration parameter $q(z)$ using all data set and how is expected our model show $q(z) < 0$ at late times and $q(z) > 0$ at earlier epoch, which means that the history of the expansion is slowed down in the past and speeded up at present with value of $q_0 = -0.582 \pm 0.059$. The transition from decelerated to accelerated phase occurs at $z \sim 0.76$. Finally, Figure (5) shows the results for jerk parameter $j(z)$ obtained from our kinematic analysis, where at later times we can appreciate a deviation from Λ CDM (dashed black curve). Although the Fluid/Gravity model is still in agreement with the standard model and the latter cannot be discarded since it is within the region of propagation of error at one sigma (gray region).

6 Conclusion

In this paper, we have used fluid/gravity duality to find a holographic dark energy model. This dark energy model was dual to a five dimensional Schwarzschild black hole. We were able to find the correct behavior for this holographic model from its dual description. We were thus able to relate the parametric space of the holographic dark energy model to its dual description. We then analyzed the thermodynamical stability of this five dimensional Schwarzschild black hole, and use the fluid/gravity duality to analyze the behavior of the

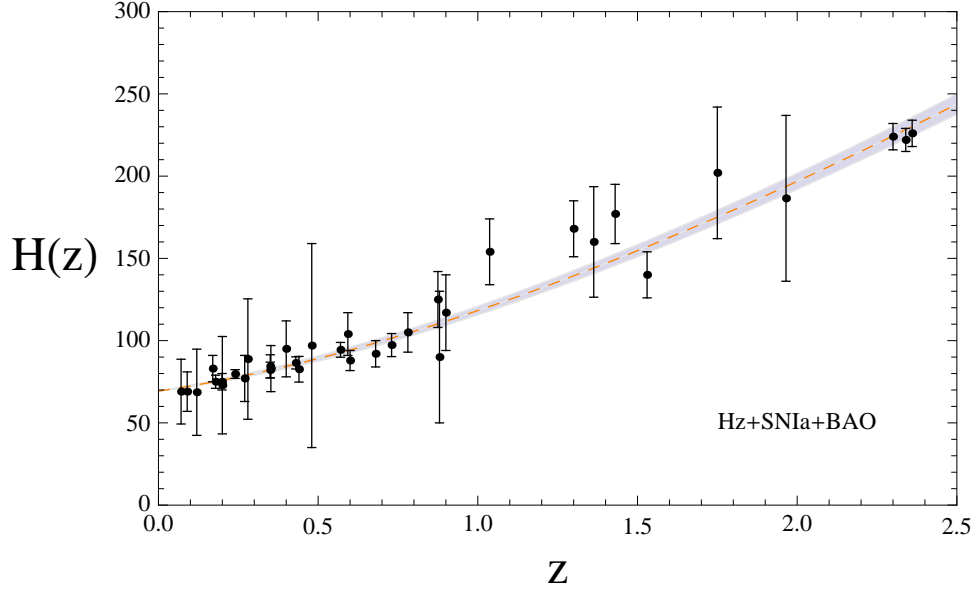


Figure 3. Using data set we plot the $H(z)$ function reconstructed using the best fit values for the $H(z) + SNIa + BAO$ case and the Observational Hubble data set . We consider the error propagation at 1σ (Gray region) in the best fit parameters (h, Ω_m, w) .

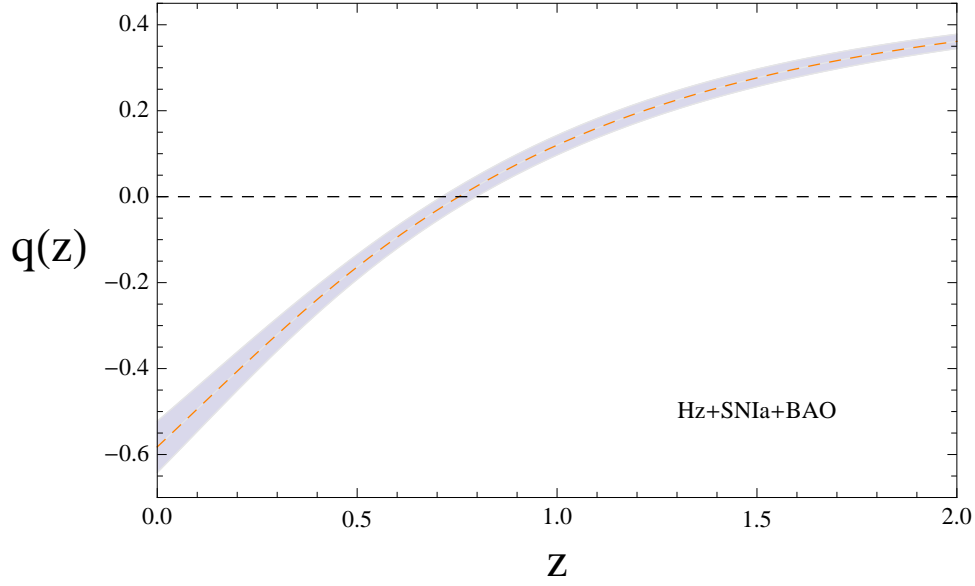


Figure 4. Using data set we plot the deceleration parameter reconstructed using the best fit values for the $H(z) + SNIa + BAO$ case. We consider the error propagation at 1σ (Gray region) in the best fit parameters (h, Ω_m, w) .

dark energy model. Finally, we used cosmological observational data to constraint the parametric space of this holographic dark energy model.

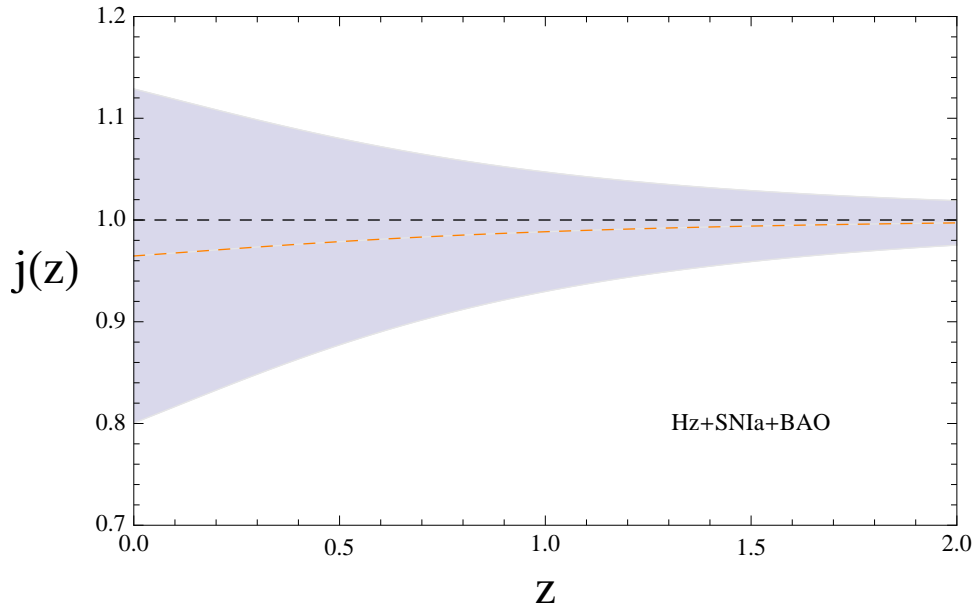


Figure 5. Using data set we plot the $j(z)$ parameter reconstructed using the best fit values for the $H(z) + SNIa + BAO$ case. We consider the error propagation at 1σ (Gray region) in the best fit parameters (h, Ω_m, w).

In this work, we analyzed a specific kind of dark energy models. It would be interesting to analyze such models using some more generalized equation of state for a dark energy model [48–50]. We also analyzed the thermodynamic stability for the dual description of this model. It would be interesting to analyze the effects of thermal fluctuations of such a dual description, and then analyze the duality using such some corrected thermodynamics. It may be noted that thermal fluctuations can change the behavior of thermodynamical systems [51–64], and so it is expected to have direct effect on the stability of this system.

It would also be interesting to analyze this holographic formalism for other models of dark energy, such as the generalized Chaplygin gas [65–67, 69, 69], generalized cosmic Chaplygin gas [70–72], modified Chaplygin gas [73–79], modified cosmic Chaplygin gas [80–83], extended Chaplygin gas [84–88]. It is expected that certain problems with certain values of parameters in this theory can be resolved by using such extended theories. It would also be interesting to analyze the holographic dual to such dark energy models, and constraint such models from observations.

7 Acknowledgments

The authors would like to thank Rafael C. Nunes for useful comments. The authors thank CNPq (Conselho Nacional de Desenvolvimento Científico e Tecnológico), Brazilian scientific support federal agency, for partial financial support, Grants numbers 302155/2015-5, 302156/2015-1 and 442369/2014-0. E.M.C.A. thanks the hospitality of Theoretical Physics

Department at Federal University of Rio de Janeiro (UFRJ), where part of this work was carried out.

References

- [1] G. 't Hooft, arXiv:gr-qc/9310026
- [2] L. Susskind, *J. Math. Phys.* **36** (1995) 6377
- [3] J. M. Maldacena, *Int. J. Theor. Phys.* **38** (1999) 1113
- [4] E. Witten, *Adv. Theor. Math. Phys.* **2** (1998) 253
- [5] S. S. Gubser, I. R. Klebanov and A. M. Polyakov, *Phys. Lett. B* **428** (1998) 105
- [6] R. A. Janik, *Prog. Theor. Phys. Suppl.* **186** (2010) 534
- [7] J. Sadeghi, et al., *AHEP* **2013** (2013) 759804
- [8] J. Sadeghi and B. Pourhassan, *JHEP* **0812** (2008) 026
- [9] T. Sakai and S. Sugimoto, *Prog. Theor. Phys.* **114** (2005) 1083
- [10] E. Katz, A. Lewandowski and M. D. Schwartz, *Phys. Rev. D* **74** (2006) 086004
- [11] J. Sadeghi, et. al., *Eur. Phys. J. C* **61** (2009) 527
- [12] J. Sadeghi, M. R. Setare and B. Pourhassan, *J. Phys. G: Nucl. Part. Phys.* **36** (2009) 115005
- [13] K. B. Fadafan, et. al., *Eur. Phys. J. C* **71** (2011) 1785
- [14] J. Sadeghi, B. Pourhassan and A. R. Amani, *Int. J. Theor. Phys.* **52** (2013) 42.
- [15] J. Sadeghi, B. Pourhassan and S. Heshmatian, *AHEP* **2013** (2013) 759804
- [16] B. Pourhassan and J. Sadeghi, *Can. J. Phys.* **91** (2013) 995
- [17] S. Sachdev, *Lect. Notes Phys.* **828** (2011) 273
- [18] S. A. Hartnoll, C. P. Herzog, G. T. Horowitz, *JHEP* **0812** (2008) 015
- [19] S. A. Hartnoll, C. P. Herzog, *Phys. Rev. D* **77** (2008) 106009.
- [20] H. Saadat and B. Pourhassan, *Int. J. Theor. Phys.* **52** (2013) 997
- [21] B. Pourhassan, M. M. Bagheri-Mohagheghi, arXiv:1609.08402 [hep-th]
- [22] M. Rangamani, *Class. Quant. Grav.* **26** (2009) 224003
- [23] C. P. Herzog, et. al., *JHEP* **0607** (2006) 013
- [24] P. S. Apostolopoulos, G. Siopsis and N. Tetradis, *Phys. Rev. Lett.* **102** (2009) 151301
- [25] M. Li, *Phys. Lett. B* **03** (2004) 1
- [26] M. Li, X. D. Li, J. Meng and Z. Zhang, *Phys. Rev. D* **88** (2013) 023503
- [27] E. N. Saridakis, *Phys. Lett. B* **661** (2008) 335
- [28] A. Mukherjee, *JCAP* **11** (2016) 055
- [29] J. F. Zhang, M. M. Zhao, Y. H. Li and X. Zhang, *JCAP* **04** (2015) 038
- [30] S. Pan and S. Chakraborty, *Int. J. Mod. Phys. D* **23** (2014) 1450092
- [31] L. P. Chimento and M. G. Richarte, *Phys. Rev. D* **85** (2012) 127301

- [32] J. M. Magán, D. Melnikov and M. R. O. Silva, *JHEP* **1411** (2014) 069
- [33] S. Bhattacharyya, V. E. Hubeny, S. Minwalla and M. Rangamani, *JHEP* **0802** (2008) 045
- [34] B. Pourhassan, E. O. Kahya, *Results Phys.* **4** (2014) 101
- [35] B. Pourhassan and E. O. Kahya, *AHEP* **2014** (2014) 231452
- [36] E. O. Kahya, B. Pourhassan, *Mod. Phys. Lett. A* **30** (2015) 1550070
- [37] E. O. Kahya and B. Pourhassan, *Astro Space Science* **353** (2014) 677
- [38] Planck Collaboration, Ade, P. A. R., N. Aghanim, et. al., *aap*, 571 (2014) A16
- [39] E. M. Barboza Jr. and F. C. Carvalho, *Phys. Lett. B*, **715** (2012) 19
- [40] N. Suzuki, et. al., *APJ*, **746** (2012) 85
- [41] R. C. Nunes and D. Pavon. *Phys. Rev. D* **91** (2015) 063526
- [42] D. J. Eisenstein, et. al., *APJ*, **633**, (2005) 560
- [43] X. L. Meng, X. Wang, S. Y. Li, and T. J. Zhang, *arXiv:1507.02517*
- [44] R. Andrae, T. Schulze-Hartung and P. Melchior, *arXiv:1012.3754*
- [45] A. Albrecht, et. al., *arXiv:0901.0721*.
- [46] L. Wolz, M. Kilbinger, J. Weller, and T. Giannantonio, *JCAP* **9** (2012) 009
- [47] Y. L. Bolotin, D. A. Erokhin and O. A. Lemets, *Phys. Uspekhi* **55** (2012) A02
- [48] A. De Felice, S. Nesseris, S. Tsujikawa, *JCAP* **1205** (2012) 029
- [49] M. Khurshudyan, et al. *Can. J. Phys.* **93** (2015) 449
- [50] J. P. de Leon, *Class. Quant. Grav.* **29** (2012) 135009
- [51] B. Pourhassan and M Faizal, *Nucl. Phys. B* **913** (2016) 834 [[arXiv:1611.00131](https://arxiv.org/abs/1611.00131)].
- [52] H. M. Sadjadi and M. Jamil, *Europhys. Lett.* **92** (2010) 69001
- [53] J. Sadeghi, et al., *Phys. Rev. D* **94** (2016) 064006
- [54] R. K. Kaul and P. Majumdar, *Phys. Rev. Lett.* **84** (2000) 5255
- [55] B. Pourhassan and M. Faizal *Phys. Lett. B* **755** (2016) 444
- [56] S. Carlip, *Class. Quant. Grav.* **17** (2000) 4175
- [57] B. Pourhassan, M Faizal, and U. Debnath, *Eur. Phys. J. C* **76** (2016) 145
- [58] S. Das, P. Majumdar and R. K. Bhaduri, *Class. Quant. Grav.* **19** (2002) 2355
- [59] M. Faizal, B. Pourhassan, *Physics Letters B* **751** (2015) 487
- [60] S. Mukherji and S. S. Pal, *JHEP* **0205** (2002) 026
- [61] B. Pourhassan and M. Faizal, *Europhys. Lett.* **111** (2015) 40006
- [62] F. Hammad and M. Faizal, *Int. J. Mod. Phys. D* **25** (2016) 1650080
- [63] J. Sadeghi, et al., *Can J Phys* **92** (2014) 1638
- [64] A. Pourdarvish, et al., *Int. J. Theor. Phys.* **52** (2013) 3560
- [65] A. R. Amani and B. Pourhassan, *Int. J. Theor. Phys.* **52** (2013) 1309
- [66] M. C. Bento, O. Bertolami, A. A. Sen, *Gen. Rel. Grav.* **35** (2003) 2063

- [67] H. Saadat and B. Pourhassan, *Int. J. Theor. Phys.* **52** (2013) 3712
- [68] M. C. Bento, O. Bertolami, A. A. Sen, *Phys. Rev. D* **66** (2002) 043507
- [69] H. Saadat and B. Pourhassan, *Int. J. Theor. Phys.* **53** (2014) 1168
- [70] W. Chakraborty, U. Debnath and S. Chakraborty, *Grav. Cosmol.* **13** (2007) 294
- [71] A. R. Amani and B. Pourhassan, *Int. J. Geo. Meth. Mod. Phys.* **11** (2014) 1450065
- [72] C. Ranjit and U. Debnath, *Astrophys. Space Sci.* **354** (2014) 651
- [73] H. Saadat and B. Pourhassan, *Astrophys. Space Sci.* **343** (2013) 783
- [74] H. B. Benaoum, *AHEP* **2012** (2012) 357802
- [75] J. Naji, B. Pourhassan and A. R. Amani, *Int. J. Mod. Phys. D* **23** (2014) 1450020
- [76] B. C. Paul, P. Thakur, A. Beesham, *Astrophys. Space Sci.* **361** (2016) 336
- [77] E. O. Kahya, et. al., *Phys. Rev. D* **92** (2015) 103511
- [78] H. B. Benaoum, *Int. J. Mod. Phys. D* **23** (2014) 1450082
- [79] D. Panigrahi and S. Chatterjee, *JCAP* **1605** (2016) 052
- [80] H. Saadat and B. Pourhassan, *Astrophys. and Space Sci.* **344** (2013) 237
- [81] J. Naji and H. Saadat, *Int. J. Theor. Phys.* **53** (2014) 1547
- [82] B. Pourhassan, *Int. J. Mod. Phys. D* **22** (2013) 1350061
- [83] J. Sadeghi, et al., *Int. J. Theor. Phys.* **53** (2014) 911
- [84] E. O. Kahya, et. al., *Eur. Phys. J. C* **75** (2015) 43
- [85] J. Sadeghi, et al., *Eur. Phys. J. Plus* **130** (2015) 84
- [86] B. Pourhassan, *Can. J. Phys.* **94** (2016) 659
- [87] M. Khurshudyan, *Astrophys. Space Sci.* **360** (2015) 44
- [88] B. Pourhassan, *Phys. of the Dark Univ.* **13** (2016) 132